Metallophysics and Advanced Technologies
Металофіз. новітні технол.
Metallofiz. Noveishie Tekhnol.
2025, vol. 47, No. 7, pp. 737–752
https://doi.org/10.15407/mfint.47.07.0737
Reprints available directly from the publisher

PACS numbers: 46.35.+z, 62.20.F-, 81.10.Jt, 81.40.Ef, 81.40.Lm, 81.70.Bt, 83.50.Uv

Study of the Low-Carbon Steel Plasticity Life During Deformation with Intermediate Heat Treatment

O. L. Haydamak, V. F. Hraniak

Vinnytsia National Agrarian University,
3 Sonyachna Str.,
UA-21008 Vinnytsia, Ukraine

Cold plastic deformation of metals leads to work hardening of the material, which increases its hardness, raises the tensile strength, and reduces significantly its plasticity and plastic viscosity. To expand the technological capabilities of cold plastic deformation of metals, such processes as wire production by drawing through multiple passes, gradually reducing the wire diameter, can utilize deformation in several stages with intermediate heat treatments (annealing). These treatments allow for recrystallization and healing of microdefects generated during the previous deformation stage. This study examines the recovery of plasticity after cold plastic deformation in two passes of low-carbon steel 08, with heating of the deformed work piece after the first pass to temperatures above the recrystallization temperature for different types of deformation. Based on the research results, a graph of the relationship between the degree of deformation and the stress-state indicator for different deformation types is constructed. A plasticity diagram for steel 08 is plotted for both the initial state and the state after intermediate heat treatment under the conditions of annealing at 690°C for one hour. Samples for compression, tension, torsion, and combined tension and torsion are prepared to implement various types of deformation. A graph is plotted showing the relationship between the utilized plasticity resource at the second deformation stage and the plasticity resource used at the first deformation stage. Patterns of recovery of the utilized plasticity resource during intermediate annealing for the simple and complex deformation types of different work

Corresponding author: Oleg Haydamak
E-mail: vntu111@gmail.com

Citation: O. L. Haydamak and V. F. Hraniak, Study of the Low-Carbon Steel Plasticity Life During Deformation with Intermediate Heat Treatment, *Metallofiz. Noveishie Tekhnol.*, **47**, No. 7: 737–752 (2025), DOI: 10.15407/mfint.47.07.0737

pieces made of steel 08 are established. As found, the deformation history has no significant effect on the recovery patterns of plasticity reserves during deformation with intermediate heat treatment of low-carbon steel 08.

Key words: low-carbon steel, plasticity, recrystallization, annealing, deformation.

Холодна пластична деформація металів приводить до наклепу матеріялу заготівки, який підвищує твердість матеріялу останньої, збільшує межу міцности, а також значно понижує пластичність і пластичну в'язкість. Для розширення технологічних можливостей холодного пластичного деформування металів для таких процесів як виготовлення дротів шляхом волочіння, за багато переходів поступово зменшуючи діяметер дроту, можна застосувати деформування за декілька етапів з проміжними термообробляннями (відпалами), завдяки яким відбувається рекристалізація та заліковування мікродефектів, що були зґенеровані на попередньому етапі деформування. В статті досліджено відновлення ресурсу пластичности після холодної пластичної деформації за два переходи маловуглецевої криці 08 під час нагрівання здеформованої заготівки після першого переходу до температур вище температури рекристалізації для різних видів деформування. За результатами досліджень побудовано графік залежности ступеня деформації від показника напруженого стану для різних видів деформування. Побудовано діяграму пластичности для криці 08 у вихідному стані та після проміжного термооброблення за режимами проміжного відпалювання за 690°C упродовж однієї години. Для реалізації різних видів деформування було виготовлено зразки для осаджування, розтягування, кручення й одночасного розтягування з крученням. Побудовано графік залежности використаного ресурсу пластичности на другому етапі деформування в залежності від використаного ресурсу пластичности на першому етапі деформування. Встановлено закономірності відновлення використаного ресурсу пластичности під час проміжного відпалювання для простих і складних видів деформування різних видів заготівок із криці 08. З'ясовано, що історія деформування не має значного впливу на закономірності відновлення запасу пластичности під час деформування з проміжним термічним обробленням маловуглецевої криці 08.

Ключові слова: маловуглецева криця, пластичність, рекристалізація, відпал, деформація.

(Received 3 March, 2025; in final version, 13 May, 2025)

1. INTRODUCTION

Examples of implementation of volumetric deformation processes show that the search for rational modes of preliminary heat treatment and plastic deformation, as well as the use of efficient lubricants allow achieving a stable course of parts treatment process [1, 2], particularly, the materials being difficult to deform and having low plasticity [3].

Of interest is the study of heat treatment influence on restoration of

deformed metal plasticity in the process of radial extrusion, which is characterized by the most rigid pattern of stress–strain state and a low value of ultimate deformation degree [4, 5]. Analysis of pre-annealing influence by used plasticity resource amount and by successive annealing on the amount of the metal plasticity reserve recovery was performed during radial extrusion of work pieces made from steel 08.

In industry, cold working of metals by pressure is widely used, because such treatment allows obtaining high-quality parts with accurate dimensions, which does not require their further treatment [6]. In addition, cold working of metals can be the only way to obtain some parts, for example, wires [7]. Wire can only be obtained by using such a cold deformation process as dragging (Fig. 1). In this process, wire *5* under the action of force *P* is pulled through hole *2*, which has an inlet cone at angle α. Thus, wire diameter decreases from diameter *D* to *d*, and its length increases significantly. This wire is made of low-carbon steel grades such as steel 05kp, 08, 10, as per DSTU B V.2.6-2:2009 standard.

It is known that cold plastic deformation of metals is characterized by increase in hardness, strength, and decrease in ductility and viscosity [8–10]. During the deformation process, intensive hardening occurs at its initial stage, and such characteristics as tensile strength $\sigma_в$ and yield strength $\sigma_{0.2}$ increase. The yield strength increases faster than the tensile strength, and with large deformations, tensile strength and yield strength equalize each other, while metal plasticity

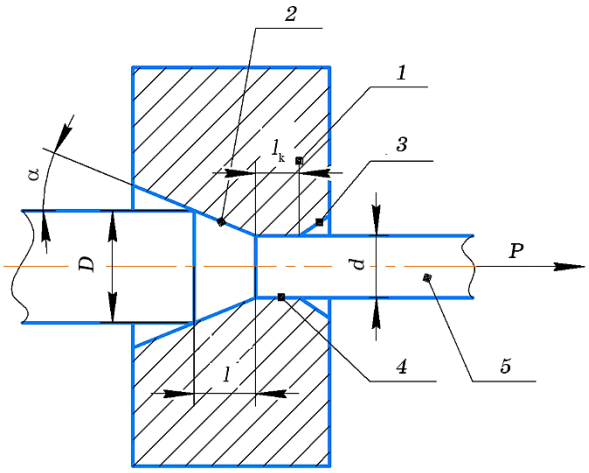

Fig. 1. Schematic representation of the process of wire production by dragging: *1*—drag, *2*—input cone, *3*—output loosening, *4*—calibration belt, *5*—wire. *P*—dragging force, *D*—initial wire diameter, *d*—post-dragging wire diameter, α—semi-angle of the input cone of the drag, *l*—length of the deformation centre section, l_k—length of the calibration belt.

drops to zero [11, 12]. Such a state of deformed material is called as the limit state, and its further deformation leads to its fracture [13, 14]. The effect of metal strengthening under the influence of cold deformation is called as hardening. Due to hardening, cold plastic deformation can increase the hardness and strength of deformed metal by 1.5 to 3 times [16, 17]. At the same time, hardening significantly reduces metals' plastic properties, which in many cases does not allow achieving the desired degree of metal deformation without exceeding its tensile strength, *i.e.*, without fracture [18]. At the same time, metal cold plastic deformation converts it into a thermodynamically unstable state, which persists indefinitely at a room temperature. Metal conversion into a more stable state is only possible by applying thermal effects to the deformed work piece [2]. Such thermal effect is called as annealing, during which the process of deformed metal recrystallization occurs. When a deformed work piece is heated, as temperature increases, there occurs increase in plasticity and decrease in strength, *i.e.*, the effect of hardening in deformed work piece disappears [19, 20]. During the recrystallization process, new grains with fewer structural defects and an equiaxed shape are formed and enlarged.

For the recrystallization to occur, certain conditions must be met, and in particular, the deformation degree must be at least 2% in low-carbon steels, 5% in iron and copper, and 6% in nickel. Moreover, for each of the above materials there exists own minimum temperature for recrystallization process T_{recr} to be started, which depends on melting temperature T_{melt} and is calculated using formula as follows [2]:

$$T_{\text{recr}} = \alpha T_{\text{melt}}, \tag{1}$$

where α is proportionality coefficient ($\alpha = 0.2$ for chemically pure metals, $\alpha = 0.4$ for technically pure alloys and metals, $\alpha = 0.8$ for complex alloys).

The recrystallization process can be described in the following sequence [21]. As the pre-treatment degree of preliminary deformation grows, the number of recrystallization centres, the so-called primary recrystallization occurs, which leads to formation of small equiaxed grains. Because of new grains' formation, hardening disappears and deformed metal plasticity of the increases. Such being the case, metal properties approach the ones existed prior to its deformation. With further heating, neighbouring grains merge and a new coarse-grained structure may appear that worsens the mechanical properties, especially, impact toughness.

Recrystallization annealing is usually used for interoperation softening of metal in the course cold dragging, rolling and other forming operations of cold pressure treatment. At enterprises, to reduce the heat treatment time, recrystallization-annealing temperature is in-

creased by 100…200°C above the recrystallization temperature.

Deformation of work pieces in several runs with annealing between runs can significantly expand technological capabilities of such processes as radial compression extrusion to obtain three and four-sided cavities, pressing, dragging and many other processes.

Heat treatment 'cures' microdefects that occur in the course of cold deformation and eliminates the hardening formed during plastic deformation. This allows for greater degrees of deformation. However, despite researchers' close attention of two studying the effect of intermediate heat treatment on plasticity, known literary sources lack data on recovery of low-carbon steels' plasticity reserve in the course of annealing and data on deformation history influence on the patterns of plasticity reserve recovery. The methodology for calculation of limit deformations during deformation with intermediate heat treatment is insufficiently substantiated.

To address these problems, experimental studies of processes of cold plastic deformation of low-carbon steel work pieces used in wire manufacture for the needs of building structures were conducted in accordance with DSTU B V.2.6-2:2009 standard. Steel 08 was chosen for the study. Specimens were prepared from steel 08 and subjected to stepwise deformation with intermediate heat treatment.

2. EXPERIMENTAL/THEORETICAL DETAILS

An important issue in development of the methodology lies in studying the influence of deformation history on recovery of work-pieces' plasticity reserve during cold deformation with intermediate annealing and, in fact, the choice of test programs. Since we are talking about plasticity under complex loading, it is necessary to implement different deformation paths. According to the linear theory of damage accumulation, the rate of damage accumulation during plastic deformation at a given time is determined by the magnitude of limiting deformation e_p. Such being the case, the rate of damage accumulation during complex deformation depends not only on the limiting deformation, but also on the 'deformation direction', which is determined by derivative $d\eta/de_u$, where η is the stress indicator and e_u is the deformation degree [6].

In order to identify this dependence influence on the regularities in plasticity reserve recovery during cold deformation with intermediate heat treatment, the basic series of experiments was carried out according to the programs corresponding to the rays emanating from ($\eta = 0$, $e_u = 0$) and ($\eta = -1$, $e_u = 0$) points. Such being the case, in the deformation vector space, the deformation path is depicted by trajectories of small curvature.

When studying the deformation history influence on recovery of

plasticity reserve of work pieces deformed with intermediate annealing, the comparison of the results of studies was carried out under simple and complex deformation.

A simple deformation will hereinafter be understood as the deformation, in which the stress state index remains unchanged throughout the deformation $\eta = \text{const}$. Complex deformation is understood as the deformation, in which the stress state index changes with the increasing deformation degree e_u [22]. Such being the case, the ratio between principal stresses and strains changes. The deformation is active (deformation with no intermediate unloading). All specimens were made of steel 08. The work pieces for the specimens were taken from one batch of metal. The specimens were brought to different stages of preliminary deformation (three specimens per stage), then annealed in an electric furnace at the temperature of 690°C with a holding time of 1 hour (cooling with the furnace) and further deformed to fracture.

To implement simple deformation, specimens were used for deposition, torsion and tension. Specimens for deposition tests had the diameter of 10 mm and the height of 16 mm (Fig. 2, *c*). The co-ordinate grid was applied to the equator of specimens' cylindrical surface using a hardness tester. The grid size was 1 mm along the equator and 2 mm along the height. Deformation was carried out on PMM-125 press. Lead foil together with graphite grease was placed under the ends of the specimens. The change in coordinate grid dimensions was measured using the instrumental microscope with the accuracy of ±0.005 mm. The moment of fracture was recorded with the appearance of the first crack with the width of 0.05 to 0.1 mm. The stress state indicator for this type of test was $\eta = -1$. The total of 12 specimens was tested.

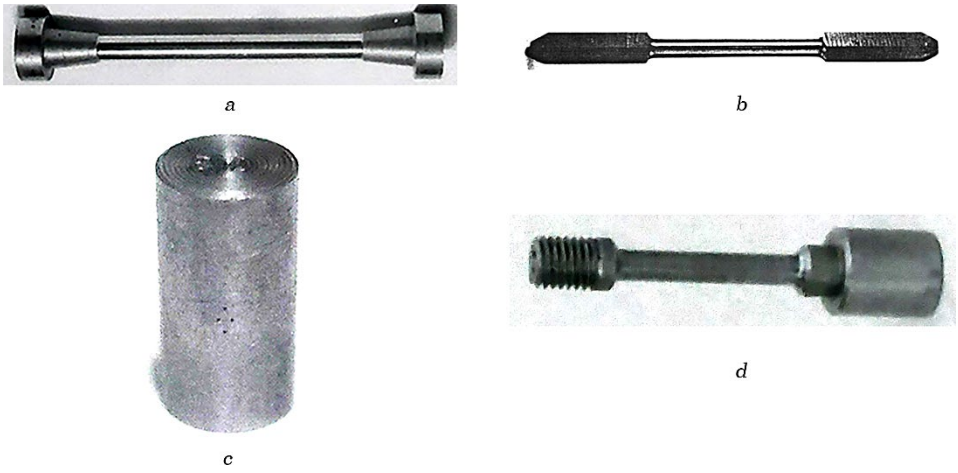

Fig. 2. General view of samples for tests on tension (*a*), torsion (*b*), deposition (*c*), and torsion with tension (*d*).

The specimens intended for testing under torsion conditions had the working part length $b = 100$ mm and diameter $d = 10$ mm (Fig. 2, *b*). A scratch was made on the working part of the specimens parallel to the generator of the working part cylinder. After the fracture, the angle of this scratch inclination relative to its initial position was measured using the instrumental microscope. The torsion test was carried out on KM-50 testing machine. The stress state indicator for this test type was $\eta = 0$. The total of 25 specimens was tested.

Specimens intended for testing under tensile conditions had working part length $L = 100$ mm and diameter $d = 10$ mm (Fig. 2, *a*). Tensile tests were carried out on P-20 testing machine. After the specimen fractured, the working part elongation and diameter were measured. The stress state index for this type of test was $\eta = 1 = \text{const}$. The total of 20 specimens was tested.

Under complex deformation conditions, deposition specimens with height $H = 16$ mm and diameter $d = 10$ mm were used (Fig. 2, *c*). Deformation was carried out without butt end lubrication. At the same time, the specimen had a convex shape on the side surface, which caused a change in the stress state index with the degree of deformation increase. The methodology of deposition tests without butt end lubrication is similar to the deposition tests with butt end lubrication, which is described above. The total of 10 specimens was tested. In addition to the specified tests, the specimens having a working part length of 30 mm and a diameter of 6 mm (Fig. 2, *d*) were deformed under conditions of joint tension and torsion. The specimens' deformation was carried out according to a given program on ZDMU-30 testing machine by smoothly increasing the twist angles and axial elongations. In this process, required elongations were controlled using a micrometer, and the twist angle was controlled using a limb installed on the testing machine.

The deformation paths under tension with torsion were defined by straight lines in $h = ke_u$ form. According to for these deformation types, the test program was calculated using formula as follows:

$$\text{tg}\alpha = z^{-1.5}\sqrt{3}\int_1^z \sqrt{z}\sqrt{\frac{1}{k^2}\left(\frac{2}{k}\ln z\right)^{-1} - 1}\,dz, \qquad (2)$$

where z is the specimen dimensionless parameter:

$$\ln z = \ln\frac{l}{l_0}, \qquad (3)$$

where l and l_0 are the specimen current and initial lengths, α is the twist angle of the initial generator on the surface of the specimen working part cylinder.

The rotation angle of one specimen end relative to the other is de-

termined by formula as follows:

$$\varphi = \frac{2l\,\mathrm{tg}\alpha}{d}\,\frac{180}{\pi}\ [\text{degrees}]. \qquad (4)$$

For the deformation types, specimens for simultaneous tension and

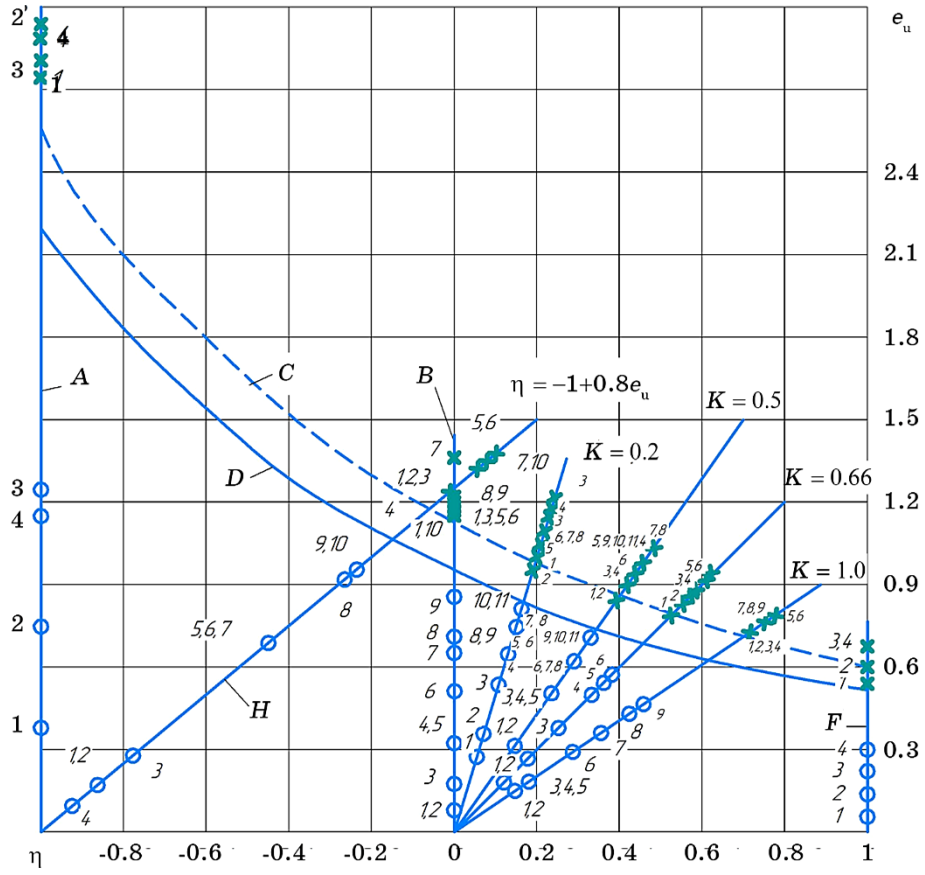

Fig. 3. Results of specimen deformation via simple and complex deformation paths with intermediate annealing: the deformation path for deposition with lubrication of the specimen butt ends (*A*), the deformation path for deposition without lubrication of the specimen butt ends (*H*), the deformation path for the specimen torsion (*B*), the deformation path for the specimen torsion with tension (*K*), the deformation path for of the specimen tensile deformation (*F*), the deformation degree (e_u), the stress state index (η), the plasticity diagram of steel 08 in the initial state (*D*), the plasticity diagram of steel 08 after annealing in intermediate heat treatment modes (*C*), the deformation degree at the first stage prior to annealing (○), the deformation degree corresponding to the specimen fracture after annealing and further deformation (×).

torsion (Fig. 3, where $K = 0.2$, 0.5, 0.66, 1.0) were used, which had working part length $L = 30$ mm and diameter $d = 6$ mm. A scratch was made on the specimen working part parallel to the generator of the working part cylinder. After fracture, the angle of this scratch inclination relative to its initial position and the specimen elongation were measured using an instrumental microscope. Test programs were calculated for these specimens, which are presented in the form of diagrams in Fig. 3. The total of 37 specimens was tested.

To assess the plasticity resource used, one should have a plasticity diagram. The plasticity diagram was constructed according to the results obtained using the following approximating expression proposed by G. D. Del [6], which includes the values of limiting deformations in torsion $e_{p(\eta=0)}$ and compression $e_{p(\eta=-1)}$ as coefficients:

$$e_p = \frac{e_{p(\eta=-1)} e_{p(\eta=0)} \exp(-\eta)}{e_{p(\eta=-1)} + \eta\left[e_{p(\eta=-1)} - e^* e_{p(\eta=0)}\right]}, \tag{5}$$

where e^* is the basis of the natural logarithm.

To these tests similarly, the tests were also conducted for annealed material in the mode corresponding to an intermediate heat treatment. Hence, two plasticity diagrams were obtained: a diagram for the material in the initial condition and the same material, but annealed in the modes corresponding to intermediate heat treatment modes.

3. RESULTS AND DISCUSSION

Obtained experimental results were processed according to the method described in Ref. [6]. During specimen deposition, the deformation degree was calculated using formula as follows:

$$e_u = \frac{2}{\sqrt{3}} \sqrt{e_z^2 + e_z e_\varphi + e_\varphi^2}, \tag{6}$$

and the stress-state index was determined using relation as follows:

$$\eta = \sqrt{3} \frac{e_z + e_\varphi}{\sqrt{e_z^2 + e_z e_\varphi + e_\varphi^2}}, \tag{7}$$

where

$$e_z = \ln \frac{z}{z_0}, \quad e_\varphi = \ln \frac{\varphi}{\varphi_0},$$

where z_0 and φ_0 are the distances between the markers in the original specimen middle zone (Fig. 2, *c*) vertically and horizontally ($z_0 = 2$ mm

and $\varphi_0 = 1$ mm, respectively); z and φ_0 are the distances between the deformed specimen same markers, vertically and horizontally, respectively.

The deformation path calculated according to these relations is shown in Fig. 3, where sign (○) indicates the annealing place and sign (×) indicates the place of the specimen fracture. The deformation path corresponding to line *A* was obtained during specimens' deposition with an intensive lubrication of the specimens' butt ends. The deformation path corresponding to line *H* was obtained, when the specimens were deposited without lubrication of the specimens' butt ends, which is described as follows:

$$\eta = -1 + 1.2 e_u . \tag{8}$$

The degree of the specimen deformation (Fig. 2, *b*) under torsion was calculated under angle α of scratch inclination on the generating cylindrical surface to its initial position, which is parallel to the specimen axis, as follows:

$$e_{u(\eta=0)} = \frac{\mathrm{tg}\alpha}{\sqrt{3}} . \tag{9}$$

The deformation path is shown in Fig. 3 (line *B*).

The deformation degree under tension was determined as follows:

$$e_{p(\eta=1)} = 2 \ln \frac{d_0}{d} , \tag{10}$$

where d_0, d are specimen diameters before and after deformation. This deformation path is shown in Fig. 3 (line *F*).

For torsion with stretching, deformation paths were constructed according to relation (1) for different values of $K = 0.2$, 0.5, 0.66 and 1.0. In Figure 3, they are marked with letter *K*.

To assess the deformation history influence on the plasticity resource recovery during annealing, one should calculate the plasticity resource used before and after annealing. For example, under torsion, tension and deposition with butt end lubrication, the resource used prior to annealing is $\Psi_1 = e_{u1}/e_{p1}$ and also after annealing $\Psi_2 = e_{u2}/e_{p2}$, where e_{p1} is the deformation degree corresponding to the fracture during the specimen deformation in the initial state before annealing, e_{p2} is the same but for the one annealed in the same conditions as during intermediate annealing. If the specimens in the initial state have no hardening, then, $e_{p1} = e_{p2}$.

When calculating Ψ_1, Ψ_2 for complex deformation (which are indicated in Fig. 3 by letters *H* and *K*), these values were determined using formula as follows [6]:

$$\Psi = \int_0^{e_u} \left(1 + 0.2\text{arctg}\frac{d\eta}{de_u}\right) \frac{e_u^{0.2\text{arctg}\frac{d\eta}{de_u}}}{\left[e_p^*(e_u)\right]^{1+0.2\text{arctg}\frac{d\eta}{de_u}}} de_u . \qquad (11)$$

In that process, the calculation was carried out similarly to the one given for simple deformation types: Ψ_1 was calculated in relation to the plasticity diagram of the material in the initial state (curve *D* in Fig. 3), and Ψ_2 was calculated in relation to the plasticity diagram of the annealed material (curve *C* in Fig. 4).

Obtained results were plotted on the graph of dependence of the plasticity resource used before and after annealing $\Psi_2 = f(\Psi_1)$ (Fig. 5). Upon processing of the results, using the least squares method and 'Trend Line' function of MS Excel program, the following expression was obtained, which approximates $\Psi_2 = f(\Psi_1)$ dependence for simple deformation types:

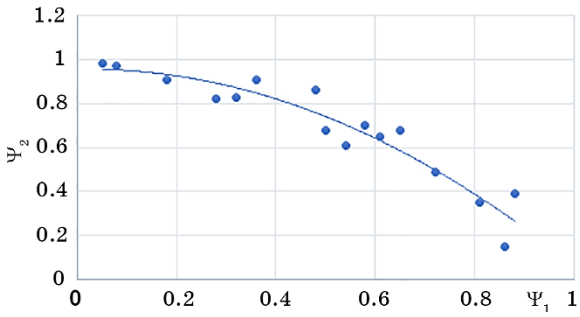

Fig. 4. Graph of dependence $\Psi_2 = f(\Psi_1)$ for simple deformation types. The following deformation types are simple: stretching where $\eta = 1 = \text{const}$, deposition where $\eta = -1 = \text{const}$, and torsion where $\eta = 0 = \text{const}$.

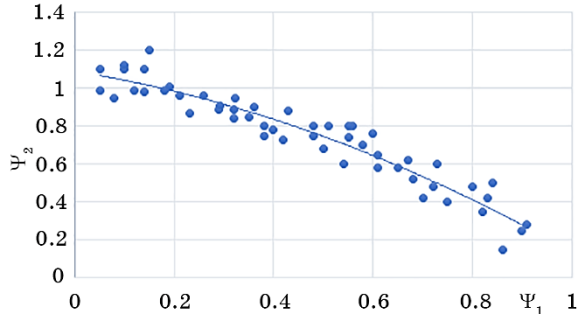

Fig. 5. Graph of dependence $\Psi_2 = f(\Psi_1)$ for complex deformation types (tension with torsion and deposition without lubrication of butt ends, where $\eta = f(e_u)$).

$$\Psi_2 = 0.9858 - 0.1169\Psi_1 - 0.8366\Psi_1^2. \quad (12)$$

The reliability of obtained approximation is $R^2 = 0.904$.

The approximation of simple deformation types is shown in Fig. 4.

The results obtained for complex deformation types were plotted on the graph of dependence of the plasticity resource used before and after annealing $\Psi_2 = f(\Psi_1)$ (Fig. 5). Upon processing of the results, using the least squares method and 'Trend Line' function of MS Excel program, the following expression was obtained, which approximates $\Psi_2 = f(\Psi_1)$ dependence for complex deformation types:

$$\Psi_2 = 1.0886 - 0.4177\Psi_1 - 0.5355\Psi_1^2. \quad (13)$$

The reliability of obtained approximation is $R^2 = 0.9082$.

To assess the deformation history influence on the process of plasticity resource recovery by intermediate annealing, let us compare the recovery results for complex and simple deformation types. To do so, using obtained approximations (12) and (13), we calculated possible plasticity resource at the second, post-annealing, deformation stage, and compared the obtained results presented in Table 1.

As can be seen from the approximations obtained for simple and complex deformation types, there are slight differences in the plasticity resource recovery Ψ_2 in the range of $0.7 \le \Psi_1 \le 0.95$ within 6.64%. At the same time, in the range of $0.2 \le \Psi_1 \le 0.7$, the results almost coincide. Hence, it can be concluded that deformation history has no significant impact on the regularities of plasticity resource recovery during deformation with intermediate annealing for simple and complex deformation types for low-carbon steel 08. Obtained results correlate well with the results obtained in the study of deformation process with intermediate annealing for high-carbon alloy steel P6M5 [6].

When designing the technological process for pressure treatment of metal with intermediate heat treatment, one should know, at what deformation stage it is advisable to perform annealing in order to achieve the desired deformation degree with no fracture. In this connection,

TABLE 1. Comparison of the results of calculation of used plasticity resource Ψ_2 for simple (by approximation (12)) and complex (by approximation (13)) deformation types with intermediate annealing.

Ψ_1	0.1	0.2	0.3	0.4	0.5	0.6	0.7	0.8	0.9
Ψ_2(12)	1.064	0.9929	0.913	0.8252	0.7288	0.6242	0.5112	0.3899	0.26
Ψ_2(13)	1.0414	0.9836	0.915	0.8358	0.7458	0.6452	0.5338	0.411	0.27
Difference	–0.022	–0.009	0.001	0.0106	0.017	0.0209	0.0225	0.021	0.01
%of deviation	–2.2	–0.9495	0.201	1.2705	2.2792	3.2517	4.2261	5.280	6.64

the method for calculation of maximum permissible deformations during deformation with intermediate heat treatment was proposed. It is known that the deformation degree that corresponds to the work-piece material fracture for different deformation types is different, while the plasticity resource used at the time of fracture for any deformation types will be the same: $\Psi = 1$.

Proceeding from these ideas, it is possible to construct a new plasticity diagram that takes into account the plasticity recovery depending on the previous deformation and annealing. For a better idea of the method for a new plasticity diagram construction, a three-dimensional diagram was used, which is shown in Fig. 7, where pre-annealing deformation degree e_{u1} is plotted on Ox-axis; the deformation degree corresponding to the fracture during post-annealing deformation e_{u2} is plotted on Oy-axis; the stress state indicator η being plotted on Oz-axis. This diagram shows the experimental values obtained under tension, compression and torsion, through which their approximating lines A, B, C are drawn. In plane (e_{u1}, η), diagram N of the initial material plasticity in the initial state is drawn. In plane (e_{u2}, η), diagram M of the initial annealed material plasticity is drawn under intermediate annealing modes.

The method for construction of a new plasticity diagram will be explained by the following example.

To do this, we will use dependence diagrams $\Psi_2 = f(\Psi_1)$ (Figs. 4, 5) and their approximations (12) and (13), which are the most accurate for simple and complex deformation types, respectively.

Knowing the plasticity resource used at the first stage, for example $\Psi_1 = 0.5$, we can, for example, determine $\Psi_2 = 0.75$ from approximation (13). The new coefficients of plasticity diagram (5) are determined from the following equation:

$$E_{p3(\eta=i)} = \Psi_1 e_{p1(\eta=i)} + \Psi_2 e_{p2(\eta=i)}; \tag{14}$$

for our example, the following values will be as follow:

$$\begin{aligned} e_{p3(\eta=1)} &= 0.5 \cdot 0.6 + 0.75 \cdot 0.7 = 0.82, \\ e_{p3(\eta=0)} &= 0.5 \cdot 1 + 0.75 \cdot 1.3 = 1.475, \\ e_{p3(\eta=-1)} &= 0.5 \cdot 2 + 0.75 \cdot 2.8 = 3.1. \end{aligned} \tag{15}$$

The discrepancy between calculation results according to the methodologies under consideration does not exceed 10%.

After the first deformation stage, the unaccounted part of used plasticity resource will be as follows:

$$\Delta\Psi_1 = 1 - \Psi_2 = 1 - 0.75 = 0.25\,. \tag{16}$$

During further deformation, calculation of used plasticity resource must be performed according to new plasticity diagram, which reflects the increase in plasticity as a result of annealing after cold deformation, *i.e.*, according to the diagram constructed according to coefficients (18). Let us assume that, at the second, post-annealing deformation stage, used plasticity resource will be $\Psi'_1 = 0.7$, and, from approximation (13), we find $\Psi'_2 = 0.53$. Then, the new coefficients of the plasticity diagram will be determined from the following equations:

$$e_{p4(\eta=i)} = e_{p2(\eta=i)}\Psi'_1 + e_{p3(\eta=i)}\Psi'_2; \tag{17}$$

$$e_{p4(\eta=1)} = 0.7 \cdot 0.7 + 0.7 \cdot 0.53 = 0.861, \tag{18}$$

$$e_{p4(\eta=0)} = 1.3 \cdot 0.7 + 1.3 \cdot 0.53 = 1.005, \tag{19}$$

$$e_{p4(\eta=-1)} = 2.8 \cdot 0.7 + 2.8 \cdot 0.53 = 2.135. \tag{20}$$

Hence, the algorithm for calculation of maximum allowable deformation degree f for several runs with intermediate annealing consists of the following stages.

1. Construction of plasticity diagrams for the work piece material in the initial state and after its annealing under the temperature modes of intermediate annealing using formula (5).
2. Construction of the deformation path for the work piece zones with the greatest deformation degree.
3. Calculation of plasticity resource Ψ_1 used at the first deformation stage.
4. Determination of possible resource Ψ_1 at the next deformation stage by approximation (12) for simple deformation paths or by approximation (13) for complex deformation types.
5. If the sum is $\Sigma(1 - \Psi_2) < 1$, it is possible to continue deformation.
6. Calculation of the plasticity-diagram new coefficients using formula (5), whose coefficients take into account plasticity recovery due to annealing. Further, the calculation takes place in a similar sequence according to paragraphs 1, 2, 3, 4.
7. If the sum is $\Sigma(1 - \Psi_2) > 1$, it is impossible to continue deformation without work piece material fracture.

This algorithm provides for the possibility of deformation in several runs until the total used plasticity resource reaches 1 and exceeds this value.

The distinctive feature of this method as compared to the method presented in paper is that the calculation of used plasticity resource is carried out taking into account the pre-annealing deformation history, while the degree of recovery of the plasticity resource used in the course of annealing is taken into account due to the rise in the plasticity diagram under the calculation method proposed. At the same time, the calculation of the plasticity resource used, as set forth in paper [4],

is performed with no regard to pre-annealing deformation history, because the deformation degree at each deformation stage is calculated from zero to the value preceding the next annealing.

4. CONCLUSION

An experimental study of the recovery of the used plasticity resource during annealing after cold plastic deformation of low-carbon steel 08 was conducted, and the results are in good agreement with the generally accepted theory of deformation. Patterns of recovery of the used plasticity resource during annealing for simple and complex deformation types of low-carbon steel were established. It was found that the type of deformation in the studied area does not significantly affect the patterns of recovery of plasticity reserves during intermediate annealing. A methodology for calculating the limiting degree of deformation in multipass deformation with intermediate annealing was developed, allowing for the consideration of the deformation history preceding each pass. It was demonstrated that the used plasticity resource, according to this methodology, was determined by considering the limiting values of the plasticity of the deformed metal, which continuously change as a result of deformations and annealing, more fully reflecting the essence of the investigated processes. The results of these studies can be applied in the development of various technological processes, such as wire production by drawing, extrusion of three- and four-cornered cavities by radial compression, axial open and closed extrusion, semi-closed extrusion, and other processes where deformation does not allow achieving the required degree of deformation in a single pass without destroying the work piece.

REFERENCES

1. S. Smirnov, *Frattura ed Integrita Strutturale*, **7**, No. 24: 7 (2013) (in Ukrainian).
2. L. M. Sokolov, I. S. Aliyev, O. Y. Markov, and L. I. Alieva, *Tekhnolohiya Kuvannya: Pidruchnyk* [Forging Technology: Textbook] (Kramatorsk: DSMA: 2011) (in Ukrainian).
3. Z. Chang and J. Chen, *Journal of Materials Processing Technology*, **276**: 116396 (2020).
4. A. A. Bogatov, C. V. Kolmogorov, and C. V. Smirnov, *Izvestiya Universiteta. Ferrous Metallurgy*, **36**, No. 2: 62 (1978) (in Ukrainian).
5. V. Borysov, A. Lytvynov, N. Braginets, A. Petryshchev, S. Artemev, B. Tsymbal, M. Poliakov, A. Bratishko, V. Kuzmenko, and O. Kholodiuk, *Eastern-European Journal of Enterprise Technologies*, **10**, No. 105: 48 (2020) (in Ukrainian).
6. O. L. Haydamak, *Metallofiz. Noveishie Tekhnol.*, **45**, No. 10: 1189 (2023) (in

Ukrainian).
7. M. Ionescu, T. Chandra, C. Sommitsch, and R. Shabadi, *Metallurgy of Steel* (Trans. Tech. Publications Ltd.: 2023).
8. E. Posviatenko, R. Posviatenko, L. Budyak, Y. Shvets, P. Paladiichuk, I. Aksom, B. Rybak, B. Sabadash, and V. Hryhoryshen, *Eastern-European Journal of Enterprise Technologies*, **12**, No. 95: 48 (2018) (in Ukrainian).
9. O. L. Haydamak and V. F. Hraniak, *Metallofiz. Noveishie Tekhnol.*, **45**, No. 12: 1485 (2023).
10. V. Hraniak, *Revue Roumaine des Sciences Techniques. Serie Electrotechnique et Energetique*, **68**, No. 4: 357 (2023) (in Ukrainian).
11. M. Ivanov, O. Pereyaslavskiy, S. Shargorodskiy, and R. Hrechko, *Journal of Physics: Conference Series*, **1741**: 012051 (2021) (in Ukrainian).
12. M. Ivanov, O. Motorna, O. Pereyaslavskyy, S. Shargorodskyi, K. Gromaszek, M. Junisbekov, A. Kalizhanova, and S. Smailova, *Mechatronic Systems. Applications in Transport, Logistics, Diagnostics, and Control* (London: Routledge: 2021).
13. V. F. Hraniak, V. V. Kukharchuk, V. V. Bilichenko, V. V. Bogachuk, S. Sh. Katsyv, S. V. Tsymbal, W. Wyjcik, and M. Kalimoldayev, *Proc. of SPIE-International Society for Optical Engineering*, **11176**: 1117663 (2019).
14. V. F. Hraniak, V. V. Kukharchuk, V. V. Bogachuk, Y. G. Vedmitskyi, I. V. Vishtak, P. Popiel, and G. Yerkeldessova, *Proc. of SPIE-International society for Optical Engineering*, **10808**: 1080866 (2018).
15. N. M. Ismail, N. A. Khatif, M. A. K. Kecik, and M. A. H. Shaharudin, *IOP Conference Series: Materials Science and Engineering*, **114**: 012108 (2016).
16. K. K. Alaneme and E. A. Okotete, *Journal of Science: Advanced Materials and Devices*, **4**, No. 1: 19 (2019).
17. S. Arafin, R. N. Singh, and A. K. George, *Phys. B: Condensed Matter*, **419**: 40 (2013).
18. I. Z. Awan and A. Q. Khan, *Journal of the Chemical Society of Pakistan*, **41**, No. 6: 1 (2019).
19. D. Arsić, V. Lazić, A. Sedmak, J. Živković, M. Djordjević, G. Mladenović *Transactions of FAMENA*, **44**, No. 2: 71 (2020) (in Croatian).
20. V. Turych, N. Weselowskaya, V. Rutkevych, and S. Shargorodskiy, *Eastern-European Journal of Enterprise Technologies*, **6**, No. 90: 60 (2017).
21. M. Pulupec and L. Shvets, *Proc. of the ICCPT-2019 Current Problems of Transport (28–29.05.2019, Ternopil, Ukraine)*, p. 195 (in Ukrainian).
22. Y. G. Vedmitskyi, V. V. Kukharchuk, V. F. Hraniak, I. V. Vishtak, P. Kacejko, and A. Abenov, *Proc. of SPIE - International Society for Optical Engineering*, **10808**: 1080801 (2018).
23. I. Kyrytsya, *Herald of Khmelnytskyi National University Technical Sciences*, **311**, No. 4: 100 (2022) (in Ukrainian).